J Mater Sci (2018) 53:15285–15297

Energy materials

New insights into chemical and electrochemical functionalization of graphene oxide electrodes by *o*-phenylenediamine and their potential applications

Denis Sačer[1], Ivan Spajić[1], Marijana Kraljić Roković[1], and Zoran Mandić[1,*]

[1] *Faculty of Chemical Engineering and Technology, University of Zagreb, Marulićev trg 19, 10000 Zagreb, Croatia*

Received: 20 February 2018
Accepted: 10 July 2018
Published online: 16 July 2018

ABSTRACT

Chemical and electrochemical functionalization of graphene oxide by *o*-phenylenediamine with its subsequent polymerization was conducted. Electrochemical functionalization was carried out by anodic oxidation of *o*-phenylenediamine on the graphene oxide-covered gold electrode, while chemical functionalization was made by incubation of graphene oxide-covered electrode in the monomer solutions of different pHs. Cyclic voltammetry with the simultaneous mass changes monitored by EQCM was used for the testing of the resulting electrodes. The results demonstrate that formation of poly (*o*-phenylenediamine) takes place not only by electrochemical oxidation of monomer but also as a result of the spontaneous heterogeneous redox reaction between oxygen functionalities on graphene oxide and *o*-phenylenediamine. Resulting composite of graphene oxide/poly(*o*-phenylenediamine) showed relatively stable response and increased currents over the wide potential range in comparison with the same polymer formed at bare gold electrode giving rise to the significant pseudocapacitance of this material. The electroactivity of the composite was preserved in neutral medium, and hydration was identified as a rate-limiting process.

Introduction

Chemical functionalization by covalent or physical attachments of molecules is a versatile method for the preparation of advanced materials and composites with tailored surfaces and improved properties for specific applications including capacitors [1, 2], sensorics [3, 4], batteries [5, 6], flexible electronics [7, 8], touch screens, light-emitting diodes, solar cells or field-effect transistors [8, 9]. Careful selection of functional molecules enables modification and precise control of the electrochemical properties of the base material.

Graphene, 2D sp^2 hybridized carbon sheet, became very popular recently as emerging material possessing remarkable mechanical [10, 11], electrical [12, 13] and thermal [14, 15], optical [16, 17] properties opening up many potential applications in diverse

Address correspondence to E-mail: zmandic@fkit.hr

https://doi.org/10.1007/s10853-018-2693-6

fields of science and technology. Low internal resistance [18] and high charge storage ability [19] attracted a huge interest for the applications of graphene-based materials in the preparation of the electrodes in supercapacitors [20, 21]. However, its widespread application is hampered by the difficulties of obtaining pure defect-free graphene sheets, their low processability and tendency of graphene to agglomerate.

Among many direct methods of the graphene synthesis such as epitaxial growth [22, 23] or chemical vapour deposition [24], chemical oxidation and exfoliation of graphite [25–27] with subsequent chemical [26, 28–30] or electrochemical reduction [31–33] of resulting graphene oxide (GO) stand out due to low price and possibility to produce large amounts of product [34–36]. Chemically obtained graphene is termed reduced graphene oxide (rGO) since residual oxygen functional groups still persist in the final product in higher or lesser extent [37–39].

Various oxygen functional groups present in rGO and GO disrupt extended π conjugation in graphene which gives unfavourable electronic effect [39–42]. The conductivity of such materials is significantly decreased compared to the pure defect-free graphene, and it is not desirable in many applications including energy storage. On the other hand, oxygen groups such as carbonyl, hydroxyl and carboxyl provide anchor sites for the chemical derivatization of graphene with various functional molecules enabling chemists to accurately control the properties of new materials by covalent or physical attachment of suitable molecules [43–46].

Conducting polymers received a lot of attention due to their interesting properties with many potential applications [47–53]. They usually have good charge storage ability, facile redox reactions and high surface area making them promising candidates for the design of active electrode materials for batteries and supercapacitors [5, 54, 55]. However, their widespread use is now limited by their unfavourable characteristics including poor chemical stability especially at high anodic potentials, dimensional instability due to heavy traffic of counter-ions and solvent molecules across the interface during charging/discharging reactions and sloping discharge profile [56]. To meet these challenges, many attempts have been made to design composite electrode materials consisting of conducting polymer with either dimensionally stable material with large surface area such as graphene or other types of pseudocapacitive materials such as transition metal oxides [6, 57–61].

In this work, we focused on the preparation of poly(*o*-phenylenediamine)/graphene oxide (PoPDA/GO) composite electrodes and on the investigation of their properties especially in the context of their application in supercapacitors. There are a couple of different approaches for the preparation of such electrodes. First, aromatic amine-based polymers can be formed either by their in situ polymerization in the presence of graphene or GO [62–65] or by anodic oxidation of *o*-PDA on the GO- or rGO-modified electrodes [62, 63]. Depending on the porosity of underlying GO, the produced electrode would rather have bilayer characteristics.

Another approach is to use various oxygen functionalities of GO for the chemical attachment of *o*-PDA monomer via its aromatic amine and its subsequent polymerization. Aromatic amines readily react with oxygen functional groups of GO producing various functional species [66–68]. *o*-PDA monomer is particularly of interest for performing these reactions since if one amine group is used for the formation of amide bonds with GO, the remaining amine could preserve extended π aromatic conjugation which is an important requisite for its oxidation followed by the polymerization. However, due to the surface confinement of this process, the resulting chain lengths are expected to be shorter compared to the PoPDA obtained by the direct anodic oxidation of monomers in solution.

Finally, there is a possibility that redox active groups at the surface of GO participate directly in the redox reaction with *o*-PDA resulting in rGO and PoPDA deposited on the electrode [67, 69, 70]. This route would be favourable from the supercapacitor application standpoint since both rGO providing high surface double layer charge and PoPDA contributing with its pseudocapacitive charge would be formed in situ in a simple one-step process [63].

There have been several attempts in the literature to synthesize GO/PoPDA composite material aimed for different applications [4, 71–73]. Lu et al. [71] reported about the preparation and supercapacitor performance of N-doped graphene using *o*-PDA as the double-N precursor. They obtained good electrochemical behaviour of the resulting material with high specific capacitance and cycling stability.

Experimental

Materials

The graphene oxide (GO—4 mg mL^{-1}) water dispersion was prepared from natural graphite powders by a Hoffman's method as described elsewhere [33, 74]. *o*-PDA (Alfa Aesar), methanol (Gram-mol), ethanol (Gram-mol), sulphuric acid (Lach-Ner), perchloric acid (Fisher Chemical) and sodium sulphate (Lach-Ner) were of analytical grade and were used without further purification.

Electrode preparations

GO-PoPDA was prepared on the quartz crystal gold electrode (RenLux Crystal Co., Ltd, China) in order to be simultaneously investigated by cyclic voltammetry and electrochemical quartz crystal microbalance (EQCM).

The gold EQCM electrodes were first washed with ethanol, acetone and bi-distilled water and after that electrochemically cycled in 0.1 mol dm^{-3} $HClO_4$ in potential range from − 0.3 to 1.3 V (vs. SCE) at 100 mV s^{-1} until a stable CV scan was achieved. An aqueous/ethanol (1:5 v/v) dispersion of pristine GO sheets (0.7 mg mL^{-1}) was prepared by sonication for 15 min. A 500 µL of obtained dispersion was spin coated on an Au EQCM electrode that was allowed to dry at room temperature and open air to form an Au/GO electrode. Mass of the GO applied on the electrode was calculated from the quartz oscillation frequency change according to the Sauerbrey equation. The currents obtained for all GO electrodes investigated in this work are expressed as specific currents, I_s/A g^{-1}, in regard to GO mass.

The incubation of *o*-PDA on the GO was carried out by immersion of Au/GO electrodes in water/methanol (9:1 v/v) (GO-PoPDA-w) or 1 mol dm^{-3} H_2SO_4 solution (GO-PoPDA-s) both containing 0.1 mol dm^{-3} of *o*-PDA monomer at room temperature (25 °C). After 24 h of incubation period, electrodes were vigorously rinsed with water and methanol and immersed for 2 h in methanol to dissolve loosely bounded monomer or possibly existing low molecular mass products. After incubation, electrodes were tested by cyclic voltammetry from − 0.2 to 0.6 V during 2 cycles and from − 0.2 to 0.8 V during 100 cycles in 1 mol dm^{-3} H_2SO_4.

Measurements

The electrochemical deposition of polymer layers either on Au (PoPDA) or Au/GO (GO-PoPDA-ec1) electrode was performed by cyclic voltammetry from 0.1 mol dm^{-3} *o*-PDA in 1 mol dm^{-3} H_2SO_4 aqueous solutions at 20 °C during 100 consecutive cycles in potential range from − 0.2 to 0.8 V at ν = 50 mV s^{-1}. Also, an experiment with Au/GO, (GO-PoPDA-ec2) electrode was performed during 200 consecutive cycles in potential range from − 0.2 to 0.3 V at ν = 50 mV s^{-1}. The usual three-electrode setup was used with EQCM Au disc (A = 1.22 cm^2) as a working electrode, saturated calomel electrode (SCE) as reference and Pt sheet as a counter electrode. All potentials in this paper are reported versus saturated calomel electrode (SCE), and experiments were carried out using potentiostat (EG&G Princeton Applied Research, model 263A).

For the EQCM measurements, the frequency of the quartz crystal coated with gold was monitored by a Stanford Research System QCM 200 quartz crystal microbalance connected to the potentiostat. The fundamental frequency was 5 MHz, and the integral sensitivity was 4.85 × 10^{-7} Hz cm^2 g^{-1}. The area of the working electrode was 1.22 cm^2 , and piezoelectrically active area was 0.427 cm^2.

FTIR-ATR spectra of prepared electrodes were recorded using a Fourier Transform-Infrared Attenuated Total Reflection PerkinElmer UATR Two spectrometer in the range 650–4000 cm^{-1}.

The UV–Vis spectra were recorded on AvaSpec-ULS2048L using UV source Model D 1000 CE, Analytical Instrument Systems Inc., USA. The samples for UV–Vis were prepared by coating of GO on a quartz slides. In order to obtain layers of GO-PoPDA-w and GO-PoPDA-s, GO/quartz layers were treated in a same way as reported for EQCM Au disc electrode.

SEM microphotographs of samples prepared on EQCM Au disc electrodes were taken by JEOL JSM 7000F at accelerating voltage of 5 kV.

Results and discussion

Mechanism of the anodic oxidation of *o*-PDA at metallic electrodes is well established and documented in the number of papers [75–79]. As shown in a set of cyclic voltammograms given in Fig. 1a, *o*-PDA oxidation at gold electrode commences at

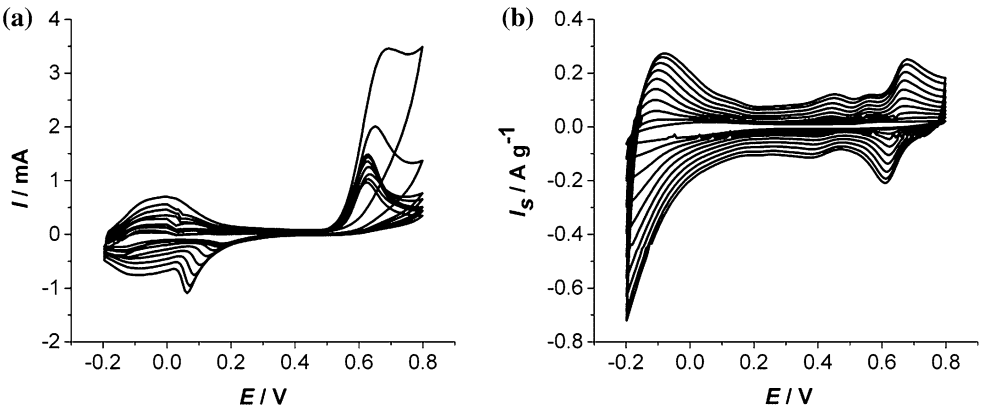

Figure 1 Cyclic voltammogram of PoPDA layer forming at **a** Au EQCM (PoPDA) and **b** GO-modified Au EQCM electrode (GO-PoPDA-ec1) during 100 consecutive cycles in 0.1 mol dm^{-3} *o*-PDA in 1 mol dm^{-3} H_2SO_4, ν = 50 mV s^{-1}.

potentials of about 0.5 V resulting in the sharp current rise. The oxidation potential of *o*-PDA is lower than the oxidation potential of aniline due to the strong positive resonance effect second amine group exerts on the aromatic ring. The oxidation current slowly decreases with the number of cycles forming one well-defined irreversible current peak at 0.612 V. The current peak height continues to decrease with the number of cycles indicating the inhibiting properties of deposited PoPDA. The rate of PoPDA formation is slower than the rate of analogous polyaniline formation probably because an autocatalytic growth is much stronger in the case of polyaniline. PoPDA redox transformations take place in the potential range from − 0.2 to 0.2 V and can be ascribed to either phenazine-like or polyaniline-like structures of the deposited polymer [4, 75, 79]. The coexistence of the two structures is also possible since at least two distinct current waves can be discerned in both cathodic and anodic potential excursions, although the two peaks are better separated and defined in cathodic regions.

When the anodic formation of PoPDA was attempted at GO-covered gold electrode, quite a different behaviour was observed on cyclic voltammograms with several distinct features (Fig. 1b). Although a negligible *o*-PDA oxidation current was observed at high anodic potentials, the formation of the PoPDA layer follows almost linear relationship with the number of cycles. In addition to the redox transformations of PoPDA which take place in the same potential range as those of the polymer layer deposited on the gold electrode, the most striking feature of the recorded cyclic voltammograms is that polymer redox transformations are not limited only to the potentials between − 0.2 and 0.2 V but almost constant oxidation/reduction current is observed throughout the whole investigated potential range. This means that the PoPDA redox sites are energetically distributed giving rise to the considerable pseudocapacitance of this material. Also, one close to reversible current peak pair appeared at potentials of about 0.7 V and the other at potential 0.45 V. The peaks remained after the electrode was transferred to the monomer-free solution indicating that they arise from the oxidation/reduction of the species firmly attached to the electrode. Since the potentials of the current peaks are much higher than those of the polymer itself, most probably they are the result of dimeric or oligomeric species of *o*-PDA.

The lack of *o*-PDA monomer oxidation current at high anodic potentials at Au/GO electrode indicates that the formation of PoPDA layer at or within GO might be a spontaneous reaction. Taking into account various redox states of oxygen functional groups at the surface of GO, the heterogeneous redox reaction between GO and *o*-PDA might occur. As a consequence, the formation of rGO and various forms of PoPDA might be expected. To test this hypothesis, the cyclic voltammetry experiment from Fig. 1b was carried out to the final potential of 0.3 V only and the results are presented in Fig. 2. The significant current increase was registered with the number of cycles especially in the potential range of PoPDA redox transformation below 0 V indicating spontaneous formation of the polymer on GO surface without initial monomer oxidation.

Additional tests were performed by immersing freshly prepared GO electrodes in the monomer solution and incubated overnight as described in the experimental section. Figure 3 shows first recorded cyclic voltammograms of two incubated electrodes, one incubated in the monomer solution of sulphuric acid (GO-PoPDA-s) and another in the water/

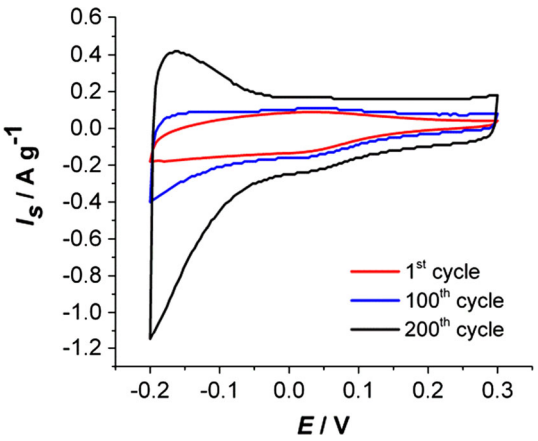

Figure 2 Cyclic voltammograms of GO-modified Au EQCM electrode (GO-PoPDA-ec2) during 200 consecutive cycles in 0.1 mol dm^{-3} *o*-PDA in 1 mol dm^{-3} H_2SO_4 in potential range up to 0.3 V where monomer electrochemical oxidation was avoided, ν = 50 mV s^{-1}.

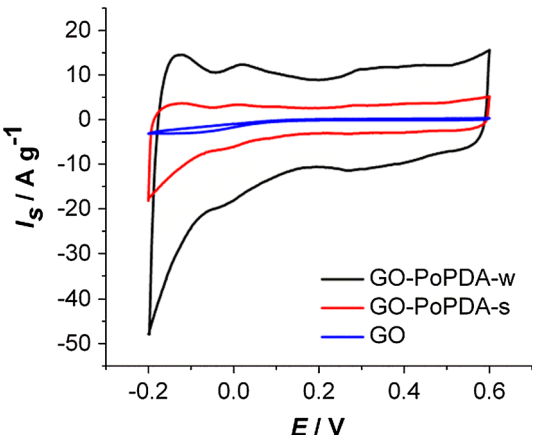

Figure 3 Cyclic voltammograms of different layers recorded in 1 mol dm^{-3} H_2SO_4, ν = 50 mVs^{-1}, after incubation period in water/methanol (GO-PoPDA-w) or sulphuric acid solution (GO-PoPDA-s).

methanol solution (GO-PoPDA-w) in comparison with the background current at GO base electrode. Obtained current profiles on cyclic voltammograms demonstrate PoPDA formation which means the layer of PoPDA was formed by chemical interaction of *o*-PDA and GO. Therefore, apart from PoPDA, reduced form of graphene (rGO) is also present at the surface of electrode. The current increase within the potential range of investigation partially should be assigned also to capacitive currents of rGO.

It looks like that PoPDA formation is favoured in neutral medium since much higher currents were registered (Fig. 3). Also, it seems that the nature of deposited polymer differs. On repetitive cycling involving anodic potentials higher than monomer oxidation potentials, the polymer formed from neutral solutions gradually dissolves or decomposes and the oxidation/reduction currents especially those below 0 V decrease (Fig. 4b), while the polymer obtained from sulphuric acid solution is not only stable at prolonged cycling but the current increases indicating additional polymer formation (Fig. 4a) although the measurements were conducted in monomer-free solution. The influence of the incubation medium on the quantity of deposited polymer might be caused by the pH dependence of the *o*-PDA oxidation potential due to the involvement of protons in the redox reaction. Chemical interaction between GO and *o*-PDA and the spontaneous PoPDA formation is thermodynamically favoured in neutral medium, and the reaction proceeds to the completion more readily than in acidic solution where a significant amount of unreacted monomer or dimeric species remained entrapped in the film and available for further electrochemical oxidation.

To confirm the existence of the spontaneous redox reaction between *o*-PDA and GO, FTIR spectra of the incubated electrodes were taken and compared to the spectra of the same electrodes after their cycling through the 100 consecutive cyclic voltammetry cycles.

The FTIR spectra of GO, GO-PoPDA-s and GO-PoPDA-w are shown in Fig. 5. The influence of pH on oxidation of *o*-PDA leads to formation of different polymer structures consisting of phenazine units or linear polymers containing free amine groups [80].

FTIR spectrum corresponding to GO shows broad absorption band in the 3600–2500 cm^{-1} region assigned to –OH stretching mode of mostly water incorporated within GO structure, but also to alkoxy groups present within the graphene structure. Characteristic absorption band for GO at 1734 cm^{-1} is assigned to carbonyl group originating from carboxyl, aldehydes or ketones. The band at 1631 cm^{-1} is assigned to asymmetric C=C stretching and –OH bending modes of water physisorbed on the GO [81]. Additional band ascribed to –OH deformation was registered at 1410 cm^{-1}. The absorption bands at 1259 cm^{-1} and 1047 cm^{-1} are commonly assigned to epoxy and alkoxy C-O stretching vibrations, respectively. After modification of GO with *o*-PDA, some of the GO bands decreased indicating removal of different oxygen groups [82], while another bands

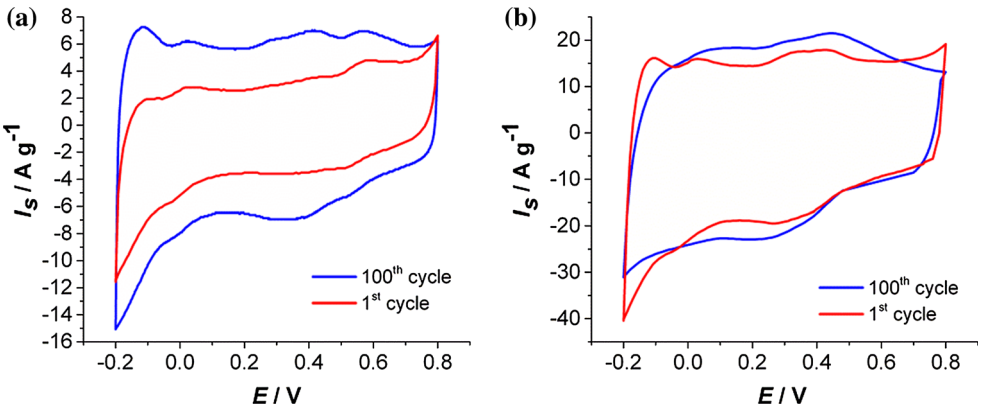

Figure 4 Cyclic voltammogram of **a** GO-PoPDA-s electrodes and **b** GO-PoPDA-w showing influence of prolonged cycling on current increase, both recorded in 1 mol dm^{-3} H_2SO_4, ν = 50 mVs^{-1}.

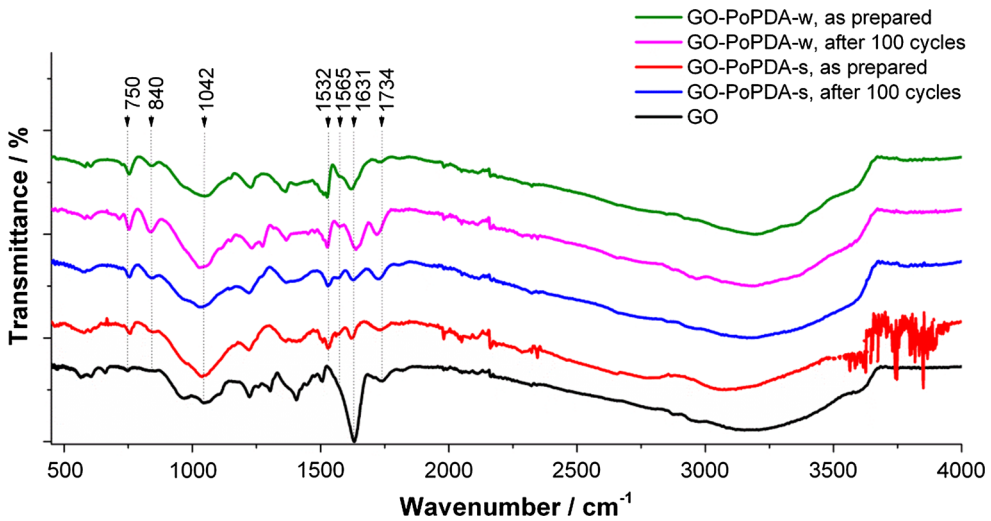

Figure 5 Comparison of FTIR spectra of GO, freshly incubated GO-PoPDA-w and GO-PoPDA-s electrodes and GO-PoPDA-w and GO-PoPDA-s electrodes polarized during 100 cycles.

appeared in spectrum after modification with *o*-PDA. The strongest peak observed in GO spectrum at 1631 cm^{-1} disappeared almost completely after incubation process and shifted towards lower wave numbers, to the value of 1620 cm^{-1}. This signifies higher symmetry of C=C bond in incubated samples indicating that during incubation process, oxygen groups responsible for asymmetric vibrations were removed [83]. Probably, process is connected with sp^2 restoration on epoxy functional groups by NH_2-group of aromatic amine which is in accordance with the literature [37]. Very weak intensity registered for bands at 1532, 1565, 750 and 840 cm^{-1} suggests the existence of low fraction of phenazine-like structure or linear-polyaniline-like structure in the film [80]. The intense band at 1532 cm^{-1} and shoulder at 1565 cm^{-1} confirm the presence of benzenoid or quinoid structures [80, 84]. The bands at 750 and 840 cm^{-1} are characteristic for out of plane C–H deformation, and it shows different coupling of the aromatic ring suggesting the presence of linear and branched structure. 1,4-coupling (polyaniline-like structure) results in 840 cm^{-1} band, and 1,3-coupling (phenazine structure) results in 750 cm^{-1} band. By comparing these two bands, it is evident that 750 cm^{-1} band was more pronounced in as-prepared GO-PoPDA-w sample in comparison with GO-PoPDA-w recorded after 100 cycles. It suggests that larger amount of the phenazine structures is present within as-prepared GO-PoPDA-w sample which is in correlation with electrochemical measurements. The intensity of these two bands was unchanged for GO-PoPDA-s before and after 100 cycles indicating stable structure with no significant change in spectrum. This is supported by cyclic voltammograms that show similar shape before and after 100 cycles.

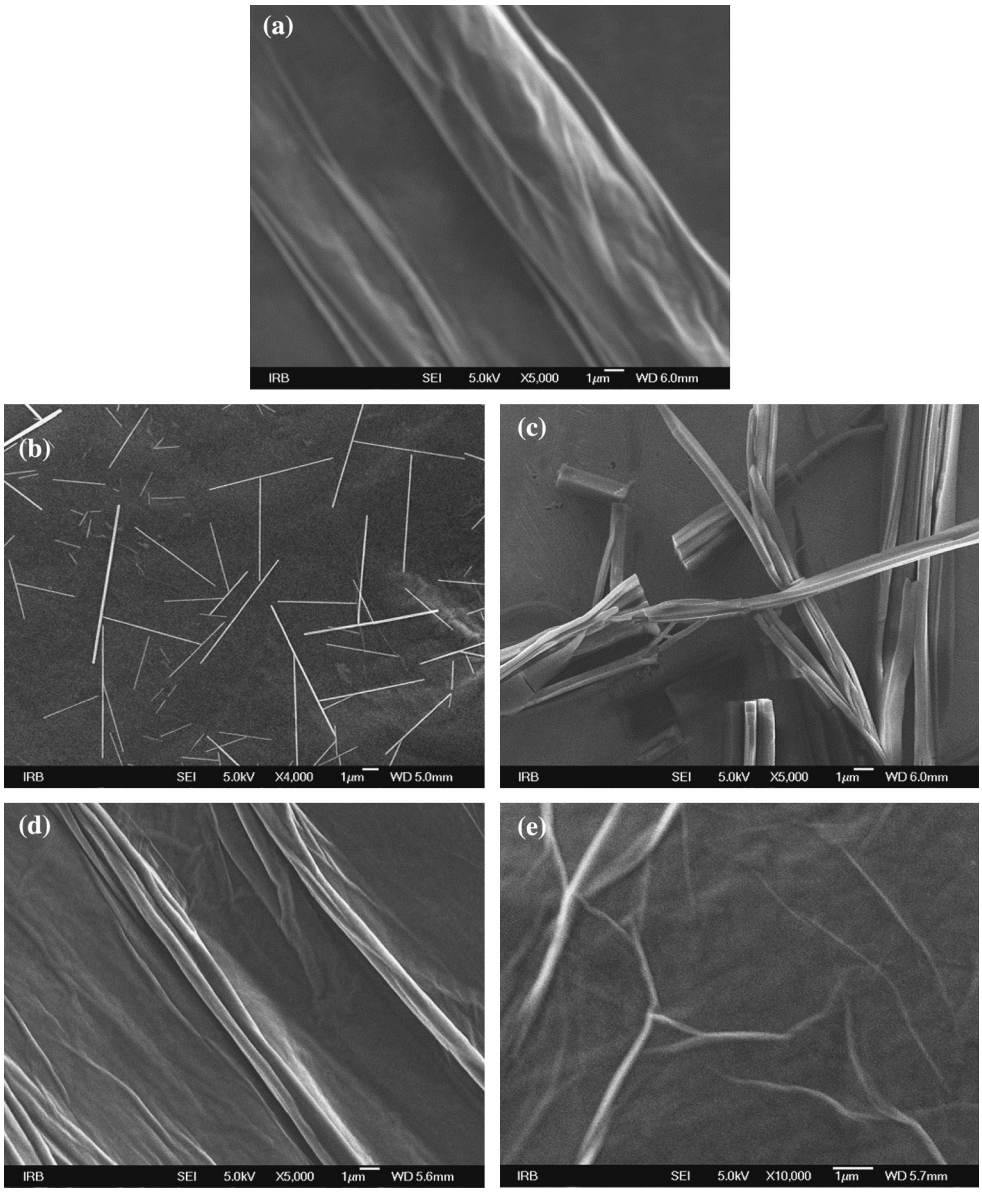

Figure 6 SEM image of **a** GO, **b** GO-PoPDA-w as-prepared, **c** GO-PoPDA-w after 100 cycle of polarization, **d** GO-PoPDA-s as-prepared, **e** GO-PoPDA-s after 100 cycle of polarization.

The band at 1042 cm^{-1} corresponds to GO structure, and therefore, by comparing the intensity of 750/840 cm^{-1} bands and 1042 cm^{-1} band, it is possible to conclude about the amount of conducting polymer within GO structure. The obtained ratio indicates that the higher amount of conducting polymer is present within the as-prepared GO-PoPDA-w compared to GO-PoPDA-w after 100 cycles. Contrary to this result, the as-prepared GO-PoPDA-s contained smaller quantity of conductive polymer. The similar observation was evident from cyclic voltammograms (Fig. 4).

The morphology of the obtained layers was investigated with SEM, and obtained micrographs are shown in Fig. 6. The surface of incubated GO-PoPDA-w is covered by a large number of uniform needles (Fig. 6b). Needle formations in the case of *o*-PDA have already been observed by other authors [85–87]. They were ascribed to low molecular mass products containing 2–7 phenazine monomer units [86]. Kar et al. [87] have also obtained low molecular mass products in the medium of higher pH values, while polymer formation ensued at pHs 1–2. After electrode cycling (Fig. 6c), the change in needle-like structures is evident. On the other hand, GO-PoPDA-s layer does not show any distinct feature different from GO (Fig. 6d, e). Since current response in the cyclic voltammograms indicates the presence of

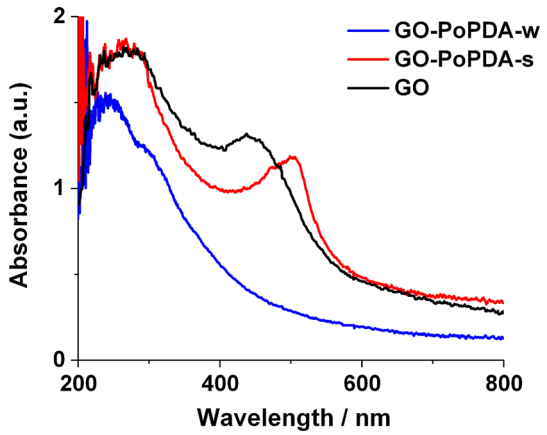

Figure 7 UV–Vis spectra of GO-covered quartz slides with subsequent incubations in sulphuric acid (red curve) and water/methanol (blue curve) monomer solution.

conducting polymer, it follows that polymer formation takes place between the GO layers and not on the outside surface of GO. This phenomenon could be related to higher solubility of *ortho*-phenylenediamine monomers or oligomers in acid medium.

UV–Vis spectroscopy was used to probe the electronic transitions in the investigated layers. The spectra of GO, GO-PoPDA-w and GO-PoPDA-s electrodes are shown in Fig. 7. Two characteristic absorption peaks were obtained for GO, the absorption maximum at 250 nm and characteristic shoulder around 300 nm. Short wavelength absorption corresponds to π–π^* transition in delocalized graphene structure, while 300 nm wavelength absorption corresponds to n–π^* transition characteristic for oxygen functionalities, and it proves the presence of oxygen within the graphene oxide structure. After modification of GO surface, the absorption maximum attributed to π–π^* transition is red-shifted from 250 to 270 nm indicating lower energy transition that is characteristic of reduced GO. It is also evident that for modified GO the characteristic shoulder at 300 nm has disappeared due to the decreased number of oxygen functionalities. For modified layers, additional absorption maximum was observed at 450 nm due to excitonic transition in quinoid-imine for GO-PoPDA-w and at 500 nm for GO-PoPDA-s due to polaronic transitions of sulphuric acid doped polymer.

Mass changes of PoPDA film at gold electrode taken during oxidation/reduction reaction are given in Fig. 8a, simultaneously with the corresponding cyclic voltammogram. The obtained mass changes were in accordance with those of PoPDA films already described in the literature [78, 79]. As demonstrated by Inzelt et al. [78], at the beginning of potential excursion, mass increase takes place which is followed by a continuous mass decrease during the rest of anodic cycle. In the range of potentials where mass increase was observed, probably some negative counter-ion influx takes place, while at later stages deprotonation of the film follows with concomitant solvent expulsion. In the reverse scan, a significant hysteresis was observed which can be explained by kinetically hindered swelling/deswelling together with the accompanying structural changes [78]. Indeed, although the overall mass change is negligible at the potentials higher than 0.3 V where no oxidation current appears, the amu values calculated from mass-charge plot (Fig. 8b) reveal that the film continues to lose weight (− 68.3). The amu values calculated from the linear segments of the mass-

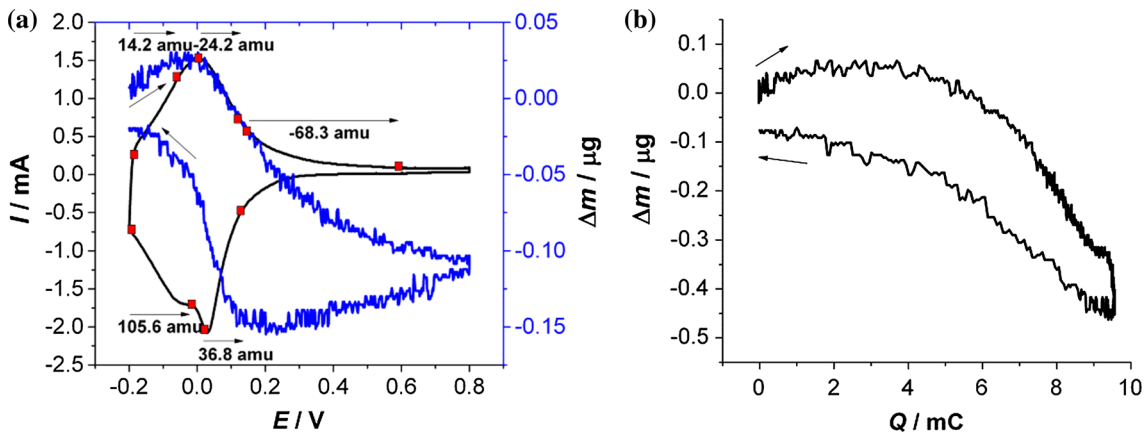

Figure 8 **a** Cyclic voltammogram and mass changes of PoPDA film at gold electrode taken during oxidation/reduction reaction and **b** corresponding mass-charge plot.

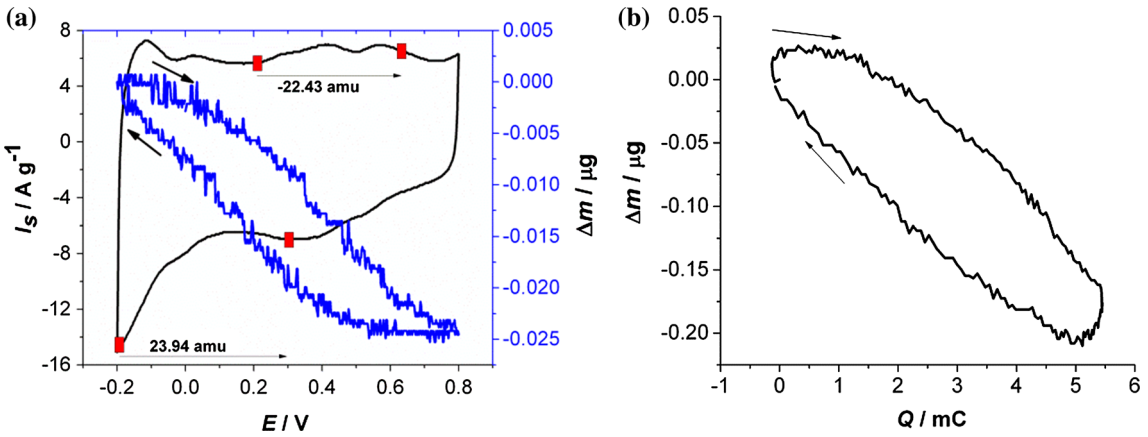

Figure 9 **a** Cyclic voltammogram of GO-PoPDA-s with corresponding EQCM mass change and **b** corresponding mass-charge plot after 100 consecutive cycles in 1 mol dm^{-3} H_2SO_4, ν = 50 mV s^{-1}.

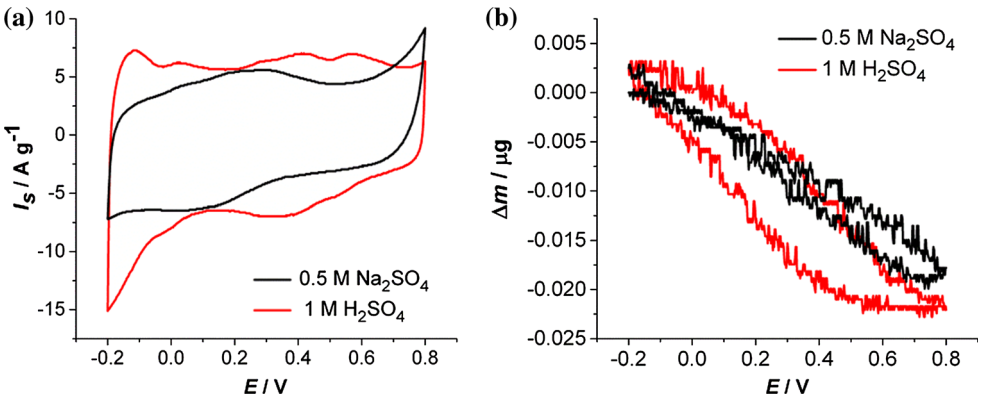

Figure 10 **a** Cyclic voltammogram of GO-PoPDA-s and **b** corresponding EQCM mass change in different electrolyte solutions, ν = 50 mVs^{-1}.

charge curves are given at the corresponding potential ranges at cyclic voltammograms (Fig. 8a).

Continuous mass decrease throughout the whole anodic potential excursion as well as mass gain in the reverse cathodic cycle was registered for the PoPDA formed on the GO support and investigated in sulphuric acid electrolyte (Fig. 9a). In Fig. 9b, corresponding mass-charge plot was displayed revealing the hysteresis similarly to the hysteresis of PoPDA film formed at gold electrode (Fig. 8a). By transferring the electrode to neutral Na_2SO_4 electrolyte, electroactivity of the film was preserved but the mass change hysteresis disappeared (Fig. 10a, b). Obviously, higher degree of reversibility was obtained in neutral medium.

The facilitated hydration of the GO-PoPDA-s film in neutral solutions is even more obvious by monitoring mass changes during several consecutive cyclic voltammetry cycles in 0.5 M Na_2SO_4 (Fig. 11). With each cycle, overall mass of the film increases but

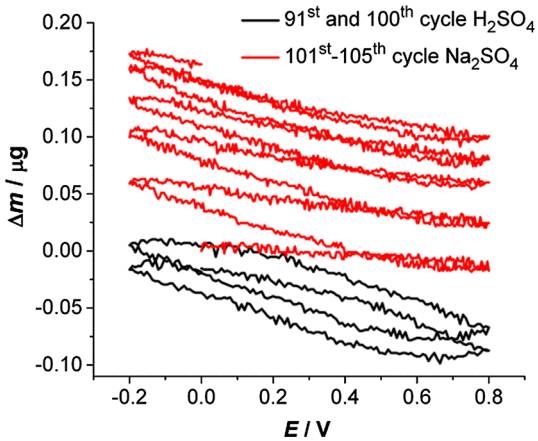

Figure 11 Corresponding EQCM mass change for GO-PoPDA-s in 1 mol dm^{-3} H_2SO_4 (black line) and 0.5 mol dm^{-3} Na_2SO_4 (red line), ν = 50 mVs^{-1}.

the increase is much more pronounced in neutral media. The hydration process might be responsible for better reversibility of redox reaction.

Conclusions

It is possible to prepare graphene oxide/poly(*o*-phenylenediamine) composite material with increased pseudocapacitive properties over the wide potential range compared to pure poly(*o*-phenylenediamine). The composite can be formed either by electrochemical oxidation of *o*-phenylenediamine on graphene oxide-covered electrode or by spontaneous heterogeneous redox reaction between graphene oxide and monomer resulting in the reduced graphene oxide and poly(*o*-phenylenediamine). The response of the composite material is stable, and the experiments demonstrated the great potentials for its utilization in supercapacitors.

Acknowledgements

The support of Croatian Science Foundation under the Project ESUP-CAP (IP-11-2013-8825) is greatly acknowledged.

References

[1] Jokar E, Shahrokhian S, Zad AI (2014) Electrochemical functionalization of graphene nanosheets with catechol derivatives as an effective method for preparation of highly performance supercapacitors. Electrochim Acta 147:136–142. https://doi.org/10.1016/j.electacta.2014.09.102

[2] Mao L, Zhang K, On Chan HS, Wu J (2012) Surfactant-stabilized graphene/polyaniline nanofiber composites for high performance supercapacitor electrode. J Mater Chem 22:80–85. https://doi.org/10.1039/C1JM12869H

[3] Zhang H, Feng J, Fei T et al (2014) SnO_2 nanoparticles-reduced graphene oxide nanocomposites for NO_2 sensing at low operating temperature. Sens Actuators B Chem 190:472–478. https://doi.org/10.1016/j.snb.2013.08.067

[4] Nguyen VH, Tran TH, Shim JJ (2014) Glassy carbon electrode modified with a graphene oxide/poly(*o*-phenylenediamine) composite for the chemical detection of hydrogen peroxide. Mater Sci Eng, C 44:144–150. https://doi.org/10.1016/j.msec.2014.08.028

[5] Sultana I, Rahman MM, Wang J et al (2012) All-polymer battery system based on polypyrrole (PPy)/para (toluene sulfonic acid) (pTS) and polypyrrole (PPy)/indigo carmine (IC) free standing films. Electrochim Acta 83:209–215. https://doi.org/10.1016/j.electacta.2012.08.043

[6] Li S, Zhu F, Meng F et al (2013) Separation of graphene oxide by density gradient centrifugation and study on their morphology-dependent electrochemical properties. J Electroanal Chem 703:135–145. https://doi.org/10.1016/j.jelechem.2013.05.020

[7] Das SR, Srinivasan S, Stromberg L et al (2017) Superhydrophobic inkjet printed flexible graphene circuits via direct-pulsed laser writing. Nanoscale 9:19058–19065. https://doi.org/10.1039/C7NR06213C

[8] Han TH, Kim H, Kwon SJ, Lee TW (2017) Graphene-based flexible electronic devices. Mater Sci Eng R Rep 118:1–43. https://doi.org/10.1016/j.mser.2017.05.001

[9] Bonaccorso F, Sun Z, Hasan T, Ferrari AC (2010) Graphene photonics and optoelectronics. Nat Photon 4:611–622. https://doi.org/10.1038/nphoton.2010.186

[10] Lee C, Wei X, Kysar JW, Hone J (2008) Measurement of the elastic properties and intrinsic strength of monolayer graphene. Science (80-) 321:385–388. https://doi.org/10.1126/science.1157996

[11] Papageorgiou DG, Kinloch IA, Young RJ (2017) Mechanical properties of graphene and graphene-based nanocomposites. Prog Mater Sci 90:75–127. https://doi.org/10.1016/j.pmatsci.2017.07.004

[12] Peres NMR, Guinea F, Castro Neto AH (2006) Electronic properties of disordered two-dimensional carbon. Phys Rev B Condens Matter Mater Phys 73:125411. https://doi.org/10.1103/PhysRevB.73.125411

[13] Neto AHC, Guinea F, Peres NMR et al (2007) The electronic properties of graphene. Rev Mod Phys 81:109–162. https://doi.org/10.1103/RevModPhys.81.109

[14] Balandin AA, Ghosh S, Bao W et al (2008) Superior thermal conductivity of single-layer graphene. Nano Lett 8:902–907. https://doi.org/10.1021/nl0731872

[15] Kim TY, Park C-H, Marzari N (2016) The electronic thermal conductivity of graphene. Nano Lett 16:2439–2443. https://doi.org/10.1021/acs.nanolett.5b05288

[16] Becerril HA, Mao J, Liu Z et al (2008) Evaluation of solution-processed reduced graphene oxide films as transparent conductors. ACS Nano 2:463–470. https://doi.org/10.1021/nn700375n

[17] Wang X, Zhi L, Müllen K (2008) Transparent, conductive graphene electrodes for dye-sensitized solar cells. Nano Lett 8:323–327. https://doi.org/10.1021/nl072838r

[18] Tsai HL, Hsieh C-T, Li J, Gandomi YA (2018) Enabling high rate charge and discharge capability, low internal resistance, and excellent cycleability for Li-ion batteries utilizing graphene additives. Electrochim Acta 273:200–207. https://doi.org/10.1016/j.electacta.2018.03.154

[19] Xia J, Chen F, Li J, Tao N (2009) Measurement of the quantum capacitance of graphene. Nat Nanotechnol 4:505–509. https://doi.org/10.1038/nnano.2009.177

[20] Stoller MD, Park S, Yanwu Z et al (2008) Graphene-based ultracapacitors. Nano Lett 8:3498–3502. https://doi.org/10.1021/nl802558y

[21] Kannappan S, Kaliyappan K, Manian RK et al (2013) Graphene based supercapacitors with improved specific capacitance and fast charging time at high current density. arXiv:1311.1548

[22] Huang H, Chen W, Chen S, Wee ATS (2008) Bottom-up growth of epitaxial graphene on 6H-SiC(0001). ACS Nano 2:2513–2518. https://doi.org/10.1021/nn800711v

[23] Xu X, Zhang Z, Dong J et al (2017) Ultrafast epitaxial growth of metre-sized single-crystal graphene on industrial Cu foil. Sci Bull 62:1074–1080. https://doi.org/10.1016/j.scib.2017.07.005

[24] Chen X, Zhang L, Chen S (2015) Large area CVD growth of graphene. Synth Met 210:95–108. https://doi.org/10.1016/j.synthmet.2015.07.005

[25] Poh HL, Šaněk F, Ambrosi A et al (2012) Graphenes prepared by Staudenmaier, Hofmann and Hummers methods with consequent thermal exfoliation exhibit very different electrochemical properties. Nanoscale 4:3515. https://doi.org/10.1039/c2nr30490b

[26] Ambrosi A, Chua CK, Bonanni A, Pumera M (2012) Lithium aluminum hydride as reducing agent for chemically reduced graphene oxides. Chem Mater 24:2292–2298. https://doi.org/10.1021/cm300382b

[27] Marcano DC, Kosynkin DV, Berlin JM et al (2010) Improved synthesis of graphene oxide. ACS Nano 4:4806–4814. https://doi.org/10.1021/nn1006368

[28] Gao X, Jang J, Nagase S (2010) Hydrazine and thermal reduction of graphene oxide: reaction mechanisms, product structures, and reaction design. J Phys Chem C 114:832–842. https://doi.org/10.1021/jp909284g

[29] Xu Y, Sheng K, Li C, Shi G (2010) Self-assembled graphene hydrogel. ACS Nano 4:4324–4330

[30] Wei M, Qiao L, Zhang H et al (2017) Engineering reduced graphene oxides with enhanced electrochemical properties through multiple-step reductions. Electrochim Acta 258:735–743. https://doi.org/10.1016/j.electacta.2017.11.120

[31] Lindfors T, Österholm A, Kauppila J, Pesonen M (2013) Electrochemical reduction of graphene oxide in electrically conducting poly(3,4-ethylenedioxythiophene) composite films. Electrochim Acta 110:428–436. https://doi.org/10.1016/j.electacta.2013.03.070

[32] Shao Y, Wang J, Engelhard M et al (2010) Facile and controllable electrochemical reduction of graphene oxide and its applications. J Mater Chem 20:743–748. https://doi.org/10.1039/B917975E

[33] Ambrosi A, Bonanni A, Sofer Z et al (2011) Electrochemistry at chemically modified graphenes. Chem A Eur J 17:10763–10770. https://doi.org/10.1002/chem.201101117

[34] Wang J, Manga KK, Bao Q, Loh KP (2011) High-yield synthesis of few-layer graphene flakes through electrochemical expansion of graphite in propylene carbonate electrolyte. J Am Chem Soc 133:8888–8891. https://doi.org/10.1021/ja203725d

[35] Zhang M, Gao B, Vanegas DC et al (2014) Simple approach for large-scale production of reduced graphene oxide films. Chem Eng J 243:340–346. https://doi.org/10.1016/j.cej.2014.01.019

[36] Huang NM, Lim HN, Chia CH et al (2011) Simple room-temperature preparation of high-yield large-area graphene oxide. Int J Nanomed 6:3443–3448. https://doi.org/10.2147/IJN.S26812

[37] Pei S, Cheng HM (2012) The reduction of graphene oxide. Carbon N Y 50:3210–3228. https://doi.org/10.1016/j.carbon.2011.11.010

[38] Xu C, Yuan RS, Wang X (2014) Selective reduction of graphene oxide. Xinxing Tan Cailiao/New Carbon Mater 29:61–66. https://doi.org/10.1016/S1872-5805(14)60126-8

[39] Solís-Fernández P, Rozada R, Paredes JI et al (2012) Chemical and microscopic analysis of graphene prepared by different reduction degrees of graphene oxide. J Alloys Compd 536:S532–S537. https://doi.org/10.1016/j.jallcom.2012.01.102

[40] Cheng M, Yang R, Zhang L et al (2012) Restoration of graphene from graphene oxide by defect repair. Carbon N Y 50:2581–2587. https://doi.org/10.1016/j.carbon.2012.02.016

[41] Araujo PT, Terrones M, Dresselhaus MS (2012) Defects and impurities in graphene-like materials. Mater Today 15:98–109

[42] Chua CK, Ambrosi A, Sofer Z et al (2014) Back cover: chemical preparation of graphene materials results in extensive unintentional doping with heteroatoms and metals (Chem Eur J 48/2014). Chem A Eur J 20:16008. https://doi.org/10.1002/chem.201490201

[43] Kuila T, Bose S, Mishra AK et al (2012) Chemical functionalization of graphene and its applications. Prog Mater Sci 57:1061–1105. https://doi.org/10.1016/j.pmatsci.2012.03.002

[44] Georgakilas V, Otyepka M, Bourlinos AB et al (2012) Functionalization of graphene: covalent and non-covalent approaches, derivatives and applications. Chem Rev 112:6156–6214. https://doi.org/10.1021/cr3000412

[45] Ioniţă M, Vlăsceanu GM, Watzlawek AA et al (2017) Graphene and functionalized graphene: extraordinary prospects for nanobiocomposite materials. Compos Part B Eng

121:34–57. https://doi.org/10.1016/j.compositesb.2017.03.031

[46] Gong X, Liu G, Li Y et al (2016) Functionalized-graphene composites: fabrication and applications in sustainable energy and environment. Chem Mater 28:8082–8118. https://doi.org/10.1021/acs.chemmater.6b01447

[47] Scrosati B (1989) Conducting polymers and their applications. Mater Sci Forum 42:207–220. https://doi.org/10.4028/www.scientific.net/MSF.42.207

[48] Wolfart F, Hryniewicz BM, Góes MS et al (2017) Conducting polymers revisited: applications in energy, electrochromism and molecular recognition. J Solid State Electrochem 21:2489–2515. https://doi.org/10.1007/s10008-017-3556-9

[49] Santana ACO, Southgate EF, Mendes JPBG et al (2014) Characterization of an HRP–AOX–polyaniline–graphite composite biosensor. J Electrochem Sci Eng 4:165–175. https://doi.org/10.5599/jese.2014.0057

[50] Popli SA, Patel UD (2015) Electrochemical decolorization of Reactive Black 5 in an undivided cell using Ti and graphite anodes: effect of polypyrrol coating on anodes. J Electrochem Sci Eng 5:145–156. https://doi.org/10.5599/jese.164

[51] Inzelt G (2017) Recent advances in the field of conducting polymers. J Solid State Electrochem 21:1965–1975. https://doi.org/10.1007/s10008-017-3611-6

[52] Inzelt G (2008) Conducting polymers: a new era in electrochemistry, 1st edn. Springer, Berlin

[53] Inzelt G (2017) Conducting polymers: past, present, future. J Electrochem Sci Eng 8:3–37. https://doi.org/10.5599/jese.448

[54] Mandić Z, Roković MK, Pokupčić T (2009) Polyaniline as cathodic material for electrochemical energy sources. The role of morphology. Electrochim Acta 54:2941–2950. https://doi.org/10.1016/j.electacta.2008.11.002

[55] Zhang J, Zhao XS (2012) Conducting polymers directly coated on reduced graphene oxide sheets as high-performance supercapacitor electrodes. J Phys Chem C 116:5420–5426. https://doi.org/10.1021/jp211474e

[56] Wang L, Ye Y, Lu X et al (2013) Hierarchical nanocomposites of polyaniline nanowire arrays on reduced graphene oxide sheets for supercapacitors. Sci Rep 3:3568. https://doi.org/10.1038/srep03568

[57] Chen S, Zhu J, Wu X et al (2010) Graphene oxide–MnO_2 nanocomposites for supercapacitors. ACS Nano 4:2822–2830. https://doi.org/10.1021/nn901311t

[58] Siwal S, Ghosh S, Nandi D et al (2017) Synergistic effect of graphene oxide on the methanol oxidation for fuel cell application. Mater Res Express 4:95306. https://doi.org/10.1088/2053-1591/aa8a88

[59] Sopcic S, Kraljic Rokovic M, Mandic Z (2012) Preparation and characterization of RuO_2/polyaniline/polymer binder composite electrodes for supercapacitor application. J Electrochem Sci Eng 14:2021–2026. https://doi.org/10.5599/jese.2012.0010

[60] Mahla DK, Bhandari S, Rahaman M, Khastgir D (2013) Morphology and cyclic voltammetry analysis of in situ polymerized polyaniline/graphene composites. J Electrochem Sci Eng 3:157–166. https://doi.org/10.5599/jese.2013.0038

[61] Zou W-J, Mo S-S, Zhou S-L et al (2011) Preparation of mesoporous carbon/polypyrrole composite materials and their supercapacitive properties. J Electrochem Sci Eng 1:67–73. https://doi.org/10.5599/jese.2011.0001

[62] Pisarevskaya EY, Ehrenburg MR, Ovsyannikova EV et al (2017) Studies of chemical stage of synthesis of electroactive composite based on poly-*o*-phenylenediamine and graphene oxide. Russ J Electrochem 53:70–77. https://doi.org/10.1134/S1023193517010104

[63] Pisarevskaya EY, Efimov ON, Ehrenburg MR, Andreev VN (2015) Preparation of electrode material with developed surface and pronounced electroactivity by modification of glassy carbon by graphene oxide and poly-*o*-phenylenediamine. Prot Met. Phys Chem Surf 51:980–984. https://doi.org/10.1134/S2070205115060180

[64] Imran SM, Kim Y, Shao GN et al (2014) Enhancement of electroconductivity of polyaniline/graphene oxide nanocomposites through in situ emulsion polymerization. J Mater Sci 49:1328–1335. https://doi.org/10.1007/s10853-013-7816-5

[65] Konwer S, Guha AK, Dolui SK (2013) Graphene oxide-filled conducting polyaniline composites as methanol-sensing materials. J Mater Sci 48:1729–1739. https://doi.org/10.1007/s10853-012-6931-z

[66] Xu LQ, Liu YL, Neoh KG et al (2011) Reduction of graphene oxide by aniline with its concomitant oxidative polymerization. Macromol Rapid Commun 32:684–688. https://doi.org/10.1002/marc.201000765

[67] Vacchi IA, Spinato C, Raya J et al (2016) Chemical reactivity of graphene oxide towards amines elucidated by solid-state NMR. Nanoscale 8:13714–13721. https://doi.org/10.1039/C6NR03846H

[68] Yang W, Zhou H, Huang Z et al (2017) In situ growth of single-stranded like poly (*o*-phenylenediamine) onto graphene for high performance supercapacitors. Electrochim Acta 245:41–50. https://doi.org/10.1016/j.electacta.2017.05.088

[69] Su C, Acik M, Takai K et al (2012) Probing the catalytic activity of porous graphene oxide and the origin of this

behaviour. Nat Commun 3:1298. https://doi.org/10.1038/ncomms2315

[70] Verma S, Mungse HP, Kumar N et al (2011) Graphene oxide: an efficient and reusable carbocatalyst for aza-Michael addition of amines to activated alkenes. Chem Commun 47:12673. https://doi.org/10.1039/c1cc15230k

[71] Lu Y, Zhang F, Zhang T et al (2013) Synthesis and supercapacitor performance studies of N-doped graphene materials using *o*-phenylenediamine as the double-N precursor. Carbon N Y 63:508–516. https://doi.org/10.1016/j.carbon.2013.07.026

[72] Mu S (2011) The electrocatalytic oxidative polymerization of *o*-phenylenediamine by reduced graphene oxide and properties of poly(*o*-phenylenediamine). Electrochim Acta 56:3764–3772. https://doi.org/10.1016/j.electacta.2011.02.061

[73] Liu X, Zhu H, Yang X (2014) An electrochemical sensor for dopamine based on poly(*o*-phenylenediamine) functionalized with electrochemically reduced graphene oxide. RSC Adv 4:3743–3749. https://doi.org/10.1039/C3RA45234D

[74] Sačer D, Čapeta D, Šrut Rakić I et al (2016) Tailoring polypyrrole supercapacitive properties by intercalation of graphene oxide within the layer. Electrochim Acta 193:311–320. https://doi.org/10.1016/j.electacta.2016.02.055

[75] Duić L, Kraljić Roković M, Mandić Z (2010) Composite layers consisting of polyaniline and poly(*o*-phenylenediamine): electrochemical deposition, electrochromic and electrocatalytic properties. Polym Sci Ser B 52:431–437. https://doi.org/10.1134/S1560090410070067

[76] Yano J (1995) Electrochemical and structural studies on soluble and conducting polymer from *o*-phenylenediamine. J Polym Sci, Part A: Polym Chem 33:2435–2441. https://doi.org/10.1002/pola.1995.080331416

[77] Ujvári M, Láng G, Inzelt G (2000) The problem of the low-frequency dispersion in the case of polymer film electrodes—an experimental impedance study on Au|poly (*o*-phenylenediamine) electrodes. Electrochem Commun 2:497–502. https://doi.org/10.1016/S1388-2481(00)00067-9

[78] Martinusz K, Czirdk E, Inzelt G (1994) Studies of the formation and redox transformation of poly (*o*-phenylenediamine) films using a quartz crystal microbalance. J Electroanal Chem 379:437–444

[79] Gharaibeh SA, El Sawy EN, Molero H, Birss VI (2013) Electrochemical and Mass Change Study of the Growth of Poly-(*o*-Phenylenediamine) Films on Au Substrates. J Electrochem Soc 160:H344–H354. https://doi.org/10.1149/2.098306jes

[80] Palys B, Bokun A, Rogalski J (2007) Poly-*o*-phenylenediamine as redox mediator for laccase. Electrochim Acta 52:7075–7082. https://doi.org/10.1016/j.electacta.2007.05.029

[81] Dimiev AM, Alemany LB, Tour JM (2013) Graphene oxide. Origin of acidity, its instability in water, and a new dynamic structural model. ACS Nano 7:576–588. https://doi.org/10.1021/nn3047378

[82] Fan X, Peng W, Li Y et al (2008) Deoxygenation of exfoliated graphite oxide under alkaline conditions: a green route to graphene preparation. Adv Mater 20:4490–4493. https://doi.org/10.1002/adma.200801306

[83] Su X, Wang G, Li W et al (2013) A simple method for preparing graphene nano-sheets at low temperature. Adv Powder Technol 24:317–323. https://doi.org/10.1016/j.apt.2012.08.003

[84] Zhang YS, Xu WH, Yao WT, Yu SH (2009) Oxidation-reduction reaction driven approach for hydrothermal synthesis of polyaniline hollow spheres with controllable size and shell thickness. J Phys Chem C 113:8588–8594. https://doi.org/10.1021/jp810491u

[85] Jiang H, Sun X, Huang M et al (2006) Rapid self-assembly of oligo(*o*-phenylenediamine) into one-dimensional structures through a facile reprecipitation route. Langmuir 22:3358–3361. https://doi.org/10.1021/la053091s

[86] Sestrem RH, Ferreira DC, Landers R et al (2010) Synthesis and spectroscopic characterization of polymer and oligomers of *ortho*-phenylenediamine. Eur Polym J 46:484–493. https://doi.org/10.1016/J.EURPOLYMJ.2009.12.007

[87] Samanta S, Roy P, Kar P (2015) Influence of pH of the Reaction Medium on the Structure and Property of Conducting Poly(*o*-Phenylenediamine). Mater Today Proc 2:1301–1308. https://doi.org/10.1016/J.MATPR.2015.07.046